OPEN

Original article

Nuclear Medicine Communications

The combination of ^{13}N-ammonia and ^{18}F-FDG whole-body PET/CT on the same day for diagnosis of advanced prostate cancer

Chang Yi[a], Donglan Yu[b], Xinchong Shi[a], Xiangsong Zhang[a], Ganhua Luo[a], Qiao He[a] and Xuezhen Zhang[a]

Purpose **The aim of the study was to evaluate the efficacy of ^{13}N-ammonia and ^{18}F-fluorodeoxyglucose (^{18}F-FDG) PET performed on the same day in the detection of advanced prostate cancer (PC) and its metastases.**

Patients and methods **Twenty-six patients with high-risk PC [Gleason score 8–10 or prostate-specific antigen (PSA) > 20 ng/ml or clinical tumor extension ≥ T2c] were recruited into the study. ^{13}N-Ammonia and ^{18}F-FDG PET/CT were performed on the same day (^{18}F-FDG followed ammonia, with an interval of a minimum of 2 h). Lesions were interpreted as positive, negative, or equivocal. Patient-based and field-based performance characteristics for both imaging techniques were reported.**

Results **There was significant correlation between ^{13}N-ammonia and ^{18}F-FDG PET/CT in the detection of primary PC ($\kappa = 0.425$, $P = 0.001$) and no significant difference in sensitivity (60.2 vs. 54.5%) and specificity (100 vs. 83.3%). The maximum standard uptake values and corresponding target-to-background ratio values of the concordantly positive lesions in prostate glands in the two studies did not differ significantly ($P = 0.124$ and 0.075, respectively). The sensitivity and specificity of PET imaging using ^{13}N-ammonia for lymph node metastases were 77.5 and 96.3%, respectively, whereas the values were 75 and 44.4% using ^{18}F-FDG. The two modalities were highly correlated with respect to the detection of lymph nodes and bone metastases.**

Conclusion **The concordance between the two imaging modalities suggests a clinical impact of ^{13}N-ammonia PET/CT in advanced PC patients as well as of ^{18}F-FDG. ^{13}N-Ammonia is a useful PET tracer and a complement to ^{18}F-FDG for detecting primary focus and distant metastases in PC. The combination of these two tracers on the same day can accurately detect advanced PC.** *Nucl Med Commun* **37:239–246**

Nuclear Medicine Communications 2016, **37**:239–246

Keywords: ^{18}F-FDG, metastasis, ^{13}N-ammonia, prostate cancer, whole-body PET/CT

Departments of [a]Nuclear Medicine and [b]Medical Equipment, the First Affiliated Hospital of Sun Yat-Sen University, Guangzhou, China

Correspondence to Xiangsong Zhang, MD, PhD, Department of Nuclear Medicine, the First Affiliated Hospital of Sun Yat-Sen University, #58, Zhongshan Er Road, Guangzhou 510080, China
Tel: +86 137 1147 1890; fax: +86 020 8775 5766/8491;
e-mail: xiaolong-4310@163.com

Received 17 September 2015 **Revised** 22 October 2015
Accepted 24 October 2015

Introduction

Prostate cancer (PC) is the most common malignancy among men in the USA, and its incidence has shown a growing trend worldwide [1]. It is clinically a heterogeneous disease characterized by an overall long natural history in comparison with other solid tumors, showing a wide spectrum of biological behavior ranging from indolent to aggressive [2]. Currently, PC is classified into three risk groups (low, intermediate, and high) on the basis of serum PSA level, Gleason score, and clinical stage. The treatment strategy and prognosis of PC is related to its risk level. Proper staging of PC is particularly important in high-risk primary disease before embarking on radical prostatectomy or radiation therapy [3]. Therefore, it is important to accurately detect tumor and estimate tumor extent in PC.

Conventional imaging studies such as transrectal ultrasound, computed tomography (CT), and MRI are currently used for the diagnosis of PC. However, they are not completely adequate for this remarkably heterogeneous disease [4,5]. In recent times, the use of PET/CT imaging in oncology has opened up a new role for molecular imaging in PC. As the most commonly used PET tracer, ^{18}F-fluorodeoxyglucose (^{18}F-FDG) has been regarded as limited in the diagnosis of PC because of ^{18}F-FDG excretion into the urinary bladder, relatively little glucose metabolism in some PC cases, and high ^{18}F-FDG accumulation in inflammatory tissues or benign prostatic hypertrophy [6,7]. However, ^{18}F-FDG PET/CT has been shown to have a relatively high sensitivity for detecting advanced PC lesions [8–11].

^{13}N-Ammonia is a useful ^{13}N-labeled PET imaging agent for assessing regional blood flow in tissues [12]. Nevertheless, as

DOI: 10.1097/MNM.0000000000000444

one of the principal products of nitrogen metabolism, ^{13}N-ammonia plays a significant role in glutamine synthesis [13] and has been used to detect some types of tumors [14]. Our recent studies have found that ^{13}N-ammonia can be taken up by some brain tumors and PC cells, which may be associated with its involvement in glutamine synthesis [15–17]. Although the utility of ^{13}N-ammonia PET/CT in the imaging of PC has been studied [17], the capability of ^{13}N-ammonia whole-body PET/CT in advanced PC and the combination of ^{13}N-ammonia and ^{18}F-FDG PET/CT for the diagnosis of advanced PC have not been reported.

In this study, we attempt to determine the value of ^{13}N-ammonia in comparison with ^{18}F-FDG PET/CT for detecting local tumors, lymph nodes (LNs), and bone metastases in advanced PC patients.

Patients and methods

Patients

Twenty-six patients (mean age: 72.2 years, range: 60–88 years) with high-risk PC were recruited from our PET center between August 2010 and November 2014. The inclusion criteria were as follows: (i) patients had to have a Gleason score 8–10 or PSA more than 20 ng/ml or clinical tumor extension more than or equal to T2c; (ii) ^{13}N-ammonia and ^{18}F-FDG imaging studies should have been performed on the same day; (iii) biopsy and pathological results were available. Patients with a history of a second cancer and those without pathology results were excluded. Detailed information of all patients is presented in Table 1.

Table 1 Patient characteristics

Patient nos	Age (years)	Serum PSA (ng/ml)	Clinical tumor stage	Gleason score	Number of LNMs	Number of BMs
1	60	205.08	T2	NA	NA	25
2	60	30.62	T3	NA	NA	Diffuse
3	78	10.91	T2	4+4	7	NA
4	74	NA	T4	4+3	1	4
5	75	68.13	T2	3+4	NA	4
6	78	42	T2	NA	NA	2
7	71	4.22	T2	4+5	NA	25
8	78	>1000	T3	4+5	NA	18
9	71	>1000	T3	4+4	NA	19
10	72	NA	T4	3+3	3	Diffuse
11	68	NA	T3	NA	NA	Diffuse
12	88	341.77	T3	NA	4	22
13	74	88.83	T3	5+4	1	NA
14	75	584.04	T4	4+5	NA	8
15	74	161.56	T4	3+4	2	NA
16	75	>1000	T3	4+3	NA	Diffuse
17	78	27.79	T2	3+4	NA	NA
18	61	>1000	T3	NA	4	21
19	70	78	T3	5+4	1	NA
20	64	137.52	T3	4+5	1	16
21	84	180.86	T2	NA	2	27
22	69	384	T2	3+5	6	1
23	65	>1000	T2	4+5	NA	Diffuse
24	77	23.05	T2	NA	NA	NA
25	68	892.18	T3	NA	NA	11
26	69	>1000	T3	3+4	8	10

BM, bone metastasis; LNM, lymph nodes metastasis.

The study was approved by the local ethics committee. All patients gave their written informed consent after receiving a detailed explanation of the study purpose and imaging procedure.

PET imaging

PET/CT imaging was performed using a Gemini GXL 16 scanner (Philips, Amsterdam, the Netherlands). All patients fasted for at least 8 h and urinated just before starting the PET/CT scan. Ammonia and ^{18}F-FDG PET/CT studies were performed on the same day (^{18}F-FDG followed ammonia, with an interval of a minimum of 2 h). The PET images were obtained from the top of the skull to the mid-thighs for 1.5 min/bed position in two-dimensional mode, reconstructed by the line of response algorithm and attenuation-corrected using CT. The scan protocol for CT was as follows: peak kilovoltage 140 kV, 180 mA/slice, thickness 5 mm, and rotation time 0.5 s.

Ten minutes after an intravenous injection of ^{13}N-ammonia (555–740 MBq) or 45–60 min after an intravenous injection of ^{18}F-FDG (5.18 MBq/kg), the PET/CT acquisition started. Images were interpreted using a Gemini workstation (Philips).

Image and data analysis

CT images without contrast enhancement were consistently available and allowed the identification of LNs and distant unrelated findings [18]. CT images (from PET/CT) were assessed by an experienced radiologist blinded to all other data. The malignant lesions were divided into LN metastasis and sclerotic and osteolytic lesions according to morphological criteria (size, shape, and regional grouping). The interpretation of PET/CT was made as a consensus reading of two nuclear medicine physicians. Each site of abnormally increased ^{13}N-ammonia and ^{18}F-FDG uptake on PET images was interpreted as positive, negative, or equivocal. For PET images, hyperactivity above background was considered a positive lesion. Negative ammonia and ^{18}F-FDG PET scans were those that did not show any activity or showed activity that was apparently lower than background. Equivocal was defined as any lesion with an activity between the two categories 'positive' and 'negative'.

Patients were monitored for at least 4 months (median: 11 months, range: 4–20 months). The lesions were classified as 'true positive' if they were positive on ^{13}N-ammonia and/or ^{18}F-FDG PET/CT and finally confirmed by CT and/or by clinical data (i.e. biopsy). Ammonia and ^{18}F-FDG PET lesions that primarily appeared to be benign and also benign on CT were considered as 'true negative' for metastases. The positive lesions on ^{13}N-ammonia or ^{18}F-FDG PET/CT but which were finally proved to be benign were considered as 'false positive'. The malignant lesions clearly confirmed

Table 2 PET results (the numbers of double-positive, double-equivocal, double-negative and discordant for each patients) of ammonia and ^{18}F-FDG PET/CT

Locations	Both positive	Both equivocal	Both negative	Discordant	Total
Local	25	0	0	1	26
Lymph node	9	2	9	6	26
Bone lesion	14	1	9	2	26
Total	48	3	18	9	78

by CT but which were negative on ^{13}N-ammonia or ^{18}F-FDG PET were considered 'false negative'.

The uptake of the lesion was evaluated by semi-quantitative analysis using the maximum standard uptake values (SUV_{max}). To determine the SUV_{max}, regions of interest (ROIs) were drawn over the abnormal lesions in ^{13}N-ammonia or ^{18}F-FDG PET images. Thereafter, a reference ROI in iliac fossa fat was chosen as a reference background ROI in both imaging modalities. Finally, the SUV_{max} of all ROIs was used for the calculation of target-to-background ratios (TBRs).

Statistical analysis

Patient-based and lesion-based analyses were performed. Data were defined as mean ± SD and were compared in different groups using the independent *t*-test. Sensitivity and specificity were calculated using data collected from PET studies. The Mann–Whitney *U*-test was used to compare quantitative variables in a paired group. The κ coefficient was calculated for comparison of two imaging modalities. Statistical analysis was performed with SPSS software (SPSS Inc., Chicago, Illinois, USA). A P value less than 0.05 was considered statistically significant.

Results

Of 26 patients, 12 (46%) had bone metastases, four (15%) had LN metastases, eight (31%) had both metastases, and two (8%) had no metastasis according to medical examinations (CT, PET/CT, biopsy, etc.) and clinical follow-up. In total, 218 bone lesions were assessed in 15 patients with a mean number of 15 bone lesions per patient (median: 11, range: 1–27). In those bone lesions, 115 were osteogenic, 98 were osteolytic, and five were hyperostosis (the benign lesions are not shown in Table 1). Five of the patients with positive PET/CT had extensive spread with countless bone metastases and therefore could not be included in the analysis. Meanwhile, 67 LNs were assessed in 18 patients, of which 40 LNs were metastases and 27 LNs were reactive lymphaden proliferation (the benign lesions are not shown in Table 1). Table 2 summarizes all PET results according to concordance for ^{13}N-ammonia and ^{18}F-FDG PET studies, and Fig. 1 shows the distribution of SUV_{max} and TBR values among lesions.

Primary tumor

Patient-based analysis

Twenty-six patients with primary tumor were detected correctly on ammonia PET imaging, but one patient was negative on ^{18}F-FDG PET imaging. Therefore, the sensitivity of ammonia was 100% and that of ^{18}F-FDG was 96.2%.

Lesion-based analysis

A total of 106 segments of prostate glands in 14 patients were analyzed. Pathology evaluation showed that 88 segments were malignant. Ammonia PET was able to identify 53 positive segments correctly, whereas 48 segments were positive on ^{18}F-FDG PET. According to the results of pathology, there were 18 true-negative results for ammonia PET and 15 true-negative results for ^{18}F-FDG PET. Hence, the sensitivity and specificity of ammonia were 60.2 and 100%, respectively, and those for ^{18}F-FDG were 54.5 and 83.3%. Figure 2 shows the ^{13}N-ammonia and ^{18}F-FDG images in one patient with primary PC and prostatitis, which were not consistent.

The SUV_{max} of the concordantly positive lesions in prostate glands on ammonia and ^{18}F-FDG PET/CT studies was 3.16 ± 1.77 and 3.82 ± 2.31, respectively. The values were not different between the two studies ($P = 0.124$). The TBR values also did not differ significantly between the two studies (6.06 ± 2.74 and 7.67 ± 3.98 on ammonia and ^{18}F-FDG PET/CT studies, respectively; $P = 0.075$). In addition, moderate agreement was found between ammonia and ^{18}F-FDG PET/CT for the detection of primary PC ($\kappa = 0.425$, $P = 0.001$).

Lymph node metastases

Patient-based analysis

The sensitivity and specificity of PET/CT in the detection of LN metastases in PC were 83.3 and 92.9% for ammonia and 83.3 and 64.3% for ^{18}F-FDG, respectively.

Lesion-based analysis

In total, 67 LNs were detected in 18 patients by PET and CT, of which 40 LNs were proven as malignant by PET/CT and clinical follow-up. Thirty-one LNs identified by ammonia PET were proven as true positive, compared with 30 LNs identified by ^{18}F-FDG PET; thus, the sensitivity and specificity of ammonia and ^{18}F-FDG were 77.5 and 96.3%, and 75 and 44.4%, respectively. Compared with ^{18}F-FDG, ^{13}N-ammonia PET/CT showed similar sensitivity but superior specificity. The SUV_{max} of positive LNs assessed by ammonia and ^{18}F-FDG was 4.50 ± 4.67 and 3.45 ± 2.04, respectively, whereas the TBR for ammonia and ^{18}F-FDG was 6.96 ± 3.39 and 7.39 ± 4.06, respectively. No significant difference was noted in SUV_{max} ($P = 0.419$) or TBR ($P = 0.775$) of the two imaging modalities for detecting LN metastases. However, fair agreement was found

Fig. 1

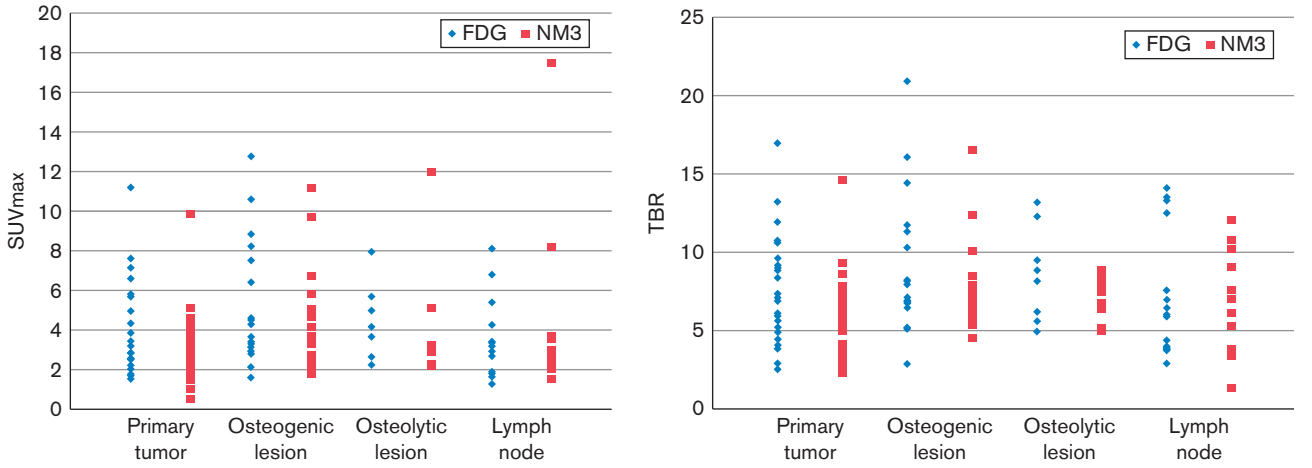

The distribution of maximum standard uptake values (SUV_{max}) and target-to-background ratio (TBR) values among lesions.

Fig. 2

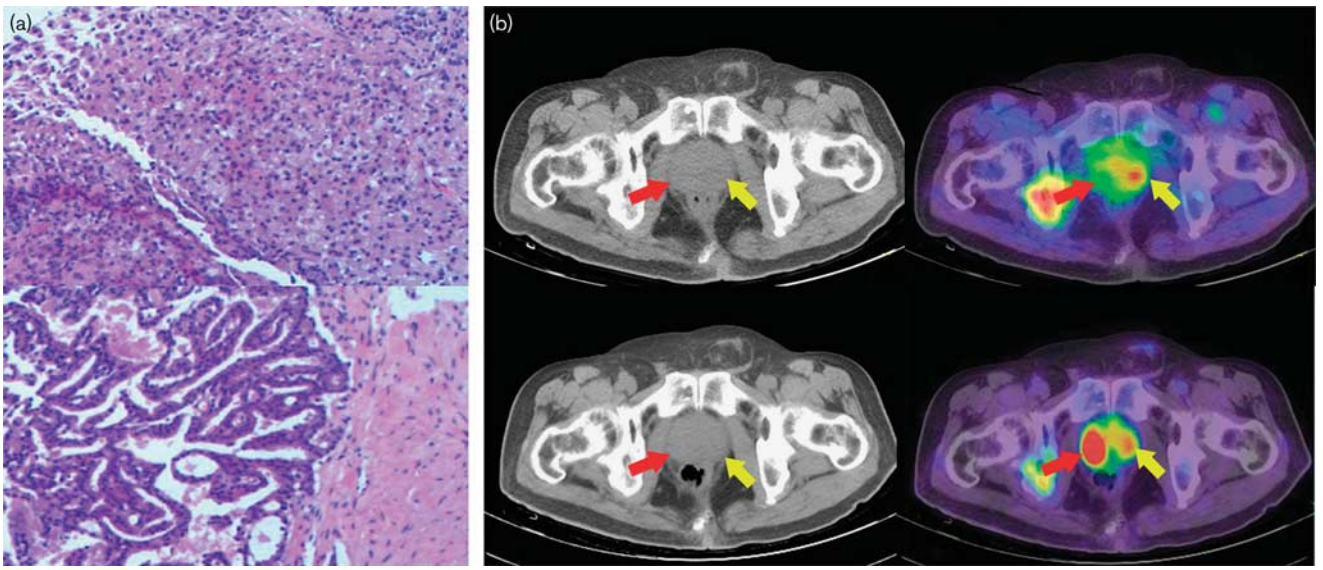

A 75-year-old man (case 5), clinical tumor stage T2, Gleason score 3 + 4, PSA 68.13 ng/ml. HE staining images (a) and PET/CT images (b) of ^{13}N-ammonia (upper row) and ^{18}F-fluorodeoxyglucose (^{18}F-FDG) (lower row) for prostatitis (red arrows) and primary prostate cancer (PC) tissues (yellow arrows). ^{13}N-Ammonia PET showed increased tracer uptake for primary PC tissues and negative for tissues prostatitis; however, ^{18}F-FDG PET were both positive. HE, hematoxylin & eosin.

between these two imaging modalities ($\kappa = 0.326$, $P = 0.003$).

Bone metastases

Patient-based analysis

Both PET/CTs were similarly positive for bone metastases in 26 patients. Only one hyperostosis patient had a positive ^{18}F-FDG PET/CT scan, whereas the corresponding ammonia PET/CT scan was negative. The sensitivity and specificity of PET/CT for the detection of bone metastases in PC were both 100% for ammonia and 100 and 83.3% for ^{18}F-FDG, respectively.

Lesion-based analysis

A total of 218 bone lesions were studied, which were divided into 115 osteogenic, 98 osteolytic, and five hyperostosis. Out of 115 osteogenic lesions, 105 (91.3%) were detected positively by ^{18}F-FDG PET/CT, compared with 112 (97.4%) by ammonia PET/CT. The SUV_{max} of positive osteogenic lesions assessed by

ammonia and ^{18}F-FDG was 4.24 ± 2.56 and 5.17 ± 3.07 ($P = 0.294$), respectively, whereas the TBR for ammonia and ^{18}F-FDG were 7.54 ± 2.85 and 9.35 ± 4.48 ($P = 0.034$), respectively. For 98 osteolytic lesions, both ammonia and ^{18}F-FDG were 100% positive. The SUV_{max} for ammonia and ^{18}F-FDG was 3.89 ± 3.16 and 4.19 ± 1.98 ($P = 0.548$), respectively, and the TBR was 6.96 ± 1.34 and 8.57 ± 3.01 ($P = 0.049$), respectively. Of five hyperostosis lesions, one was positively identified (SUV_{max}: 3.15) by ammonia PET/CT and two (SUV_{max}: 2.45, 3.06) by ^{18}F-FDG PET/CT. Furthermore, a relatively close agreement was found between ammonia and ^{18}F-FDG PET/CT for the detection of metastatic bone disease in PC patients ($\kappa = 0.589$, $P < 0.001$).

Discussion

Molecular imaging has been adopted in recent PC studies as it is a noninvasive diagnostic modality that allows accurate management of the disease [5–10]. PET/CT as one of the most important molecular imaging modalities is fundamentally suited for the imaging evaluation of biologic targets and events [5], which has been widely applied in clinical practice for examination of PC biology. As the most common PET tracer, ^{18}F-FDG may enhance the staging of advanced PC [6–9]. Generally, high uptake of ^{18}F-FDG is expected in prostate tumors that are poorly differentiated, are hypoxic, and have a high Gleason score [7]. Many different PET radiotracers are likely to be suited to various clinical states of PC, such as ^{11}C-methionine, ^{11}C-choline or ^{18}F-choline, and ^{11}C-acetate [10,18–20]. Furthermore, we found that ^{13}N-ammonia uptake in PC segments is significantly higher than that in benign segments [17], which was related to the expression of glutamine synthetase (GS) in PC. However, the previous research only studied the uptake of ^{13}N-ammonia in the pelvis. To our knowledge, the present study provided a systematic comparison of ^{13}N-ammonia and ^{18}F-FDG whole-body PET/CT for advanced PC.

The biologic mechanisms for the accumulation of ammonia are not yet clear, but there is a reasonable explanation for its use in PC. Generally, glutamine is conditionally essential in cancer cells, being utilized as an alternative fuel source to glucose for the tricarboxylic acid cycle, and as a source of fatty acid production through reductive carboxylation [21–23]. Some authors have reported that abnormal glutamine metabolism has been found in PC [24,25]. According to Cooper [13], ammonia can act as a source of glutamine in the glutamine cycle. Nevertheless, our recent studies found that ^{13}N-ammonia could also be obviously taken up by PCs; the mechanism might be associated with upregulation of de-novo glutamine synthesis in tumors [17]. Therefore, ammonia might play a significant role in glutamine synthesis.

Fig. 3

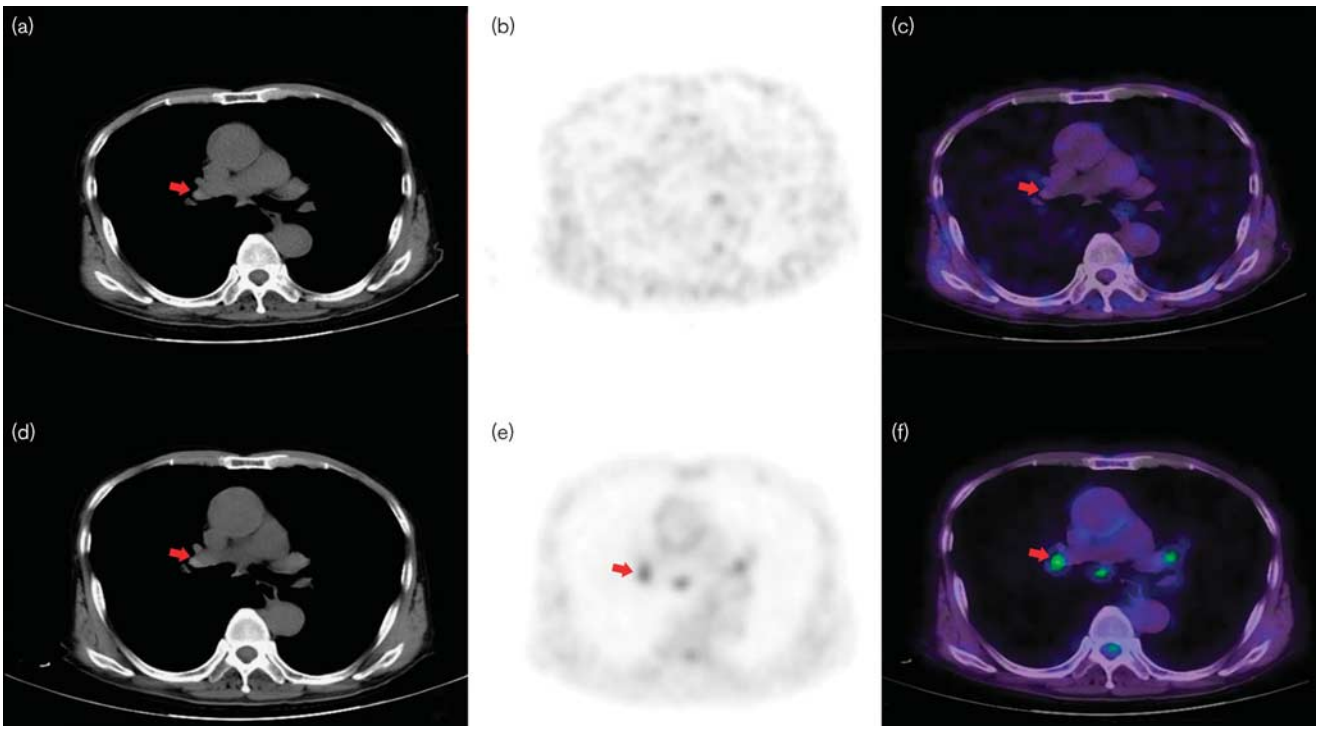

Case 24, transaxial images of ^{13}N-ammonia PET/CT (a–c) and ^{18}F-fluorodeoxyglucose (^{18}F-FDG) PET/CT (d–f) for hilar lymph node inflammation. ^{13}N-Ammonia was negative while ^{18}F-FDG PET showed increased uptake (red arrows).

At the time of ^{18}F-FDG PET, nearly 3 h had passed since the intravenous injection of ^{13}N-ammonia. Meanwhile, because of the short half-life of ^{13}N and urine excretion, ^{13}N-ammonia had already cleared from the body. Therefore, it would have had no effect on the two PET studies, and it enabled the study of ^{13}N-ammonia and ^{18}F-FDG PET on the same day. Ultimately, it was beneficial for the patients, as they did not have to travel to our PET center twice.

In this study, ammonia PET revealed all pathological lesions in the prostate in 26 patients, whereas ^{18}F-FDG PET failed in one patient. However, ammonia PET gave 53 true-positive results in 106 segments and ^{18}F-FDG PET gave 48 true-positive results. Ammonia PET had a sensitivity and specificity of 60.2 and 100%, respectively, for detecting primary PC. The sensitivity and specificity of ^{18}F-FDG PET were 54.5 and 83.3%, respectively. Shiiba *et al.* [10] reported that the sensitivity and specificity of ^{11}C-methionine for distinguishing between patients with no Gleason score and those with low-to-high Gleason scores were 78.7 and 75.6%, respectively. The sensitivity was not high for ammonia and ^{18}F-FDG for the diagnosis of primary PC. It has been reported that the usefulness of ^{18}F-FDG PET for locally prostatic neoplasms and pelvic LN metastases is limited because of bladder urine activity [7,8]. ^{13}N-Ammonia was cleared from the body primarily through the renal system [26], which also affected its interpretation of the pelvic lesions.

However, ^{13}N-ammonia could be more effective than ^{18}F-FDG in distinguishing PC from prostatitis. In a 75-year-old patient with both prostatitis and PC, both positive ^{18}F-FDG could be found in those segments, whereas prostatitis showed an absence or lower uptake of ^{13}N-ammonia (Fig. 2). One possible reason is that GS is more active in PC than in prostatitis. The combination of ammonia and ^{18}F-FDG could be helpful for the detection of PC.

When assessing LN metastasis, ^{13}N-ammonia PET showed 77.5% sensitivity versus 75% sensitivity for ^{18}F-FDG PET, but it exhibited 96.3% specificity compared with 44.4% for ^{18}F-FDG PET. (Figure 3 shows the hilar LN inflammation detected by both modalities, and Fig. 4 shows LNs and bone metastases.) Likewise, ^{13}N-ammonia PET had higher specificity than ^{18}F-FDG PET in detecting primary PC (100 vs. 83.3%). These results were consistent with our previous studies [17]. GS could be inactivated by reactive oxygen species in the macrophages [27]. Therefore, an absence or

Fig. 4

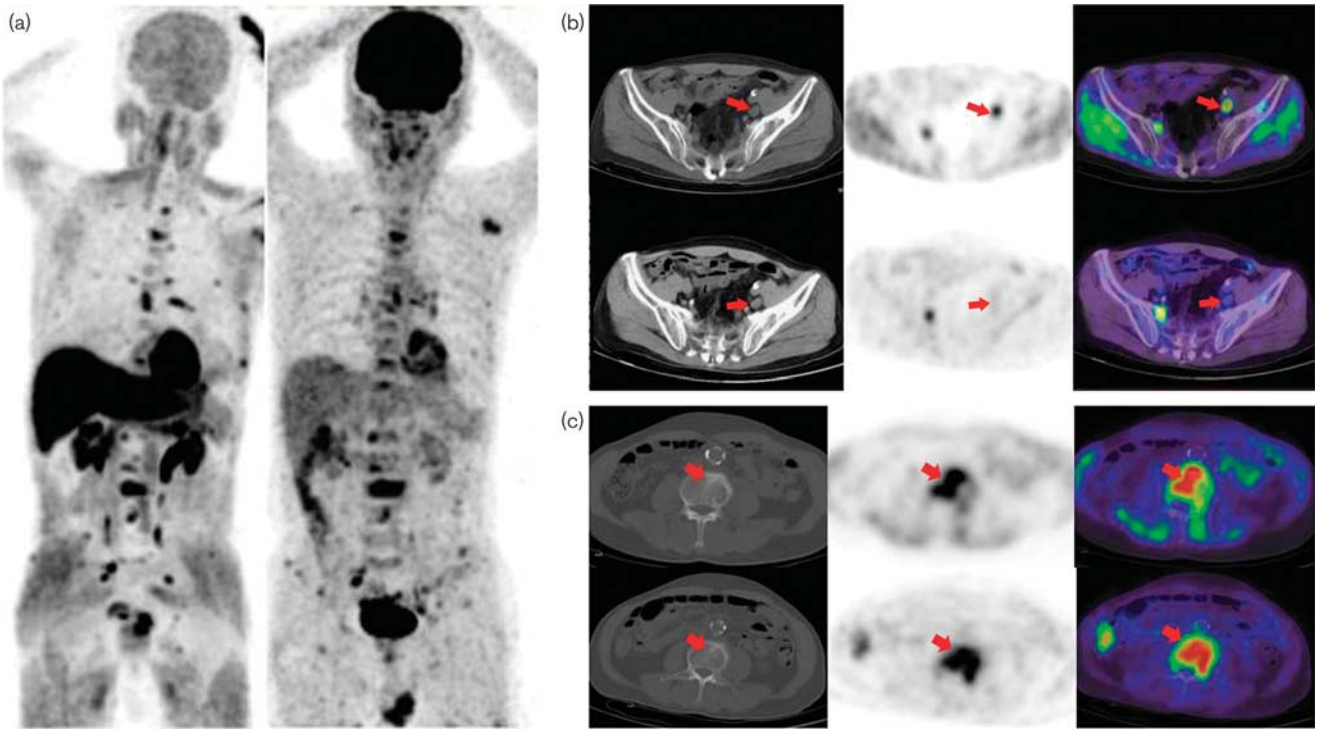

A 64-year-old prostate cancer patient (case 20) with lymph nodes and bone metastases: (a) whole-body anterior maximal intensity projection images of ^{13}N-ammonia PET/CT (left column) and ^{18}F-fluorodeoxyglucose (^{18}F-FDG) PET/CT (right column); (b) transaxial images of ammonia PET/CT (upper row) and ^{18}F-FDG PET/CT (lower row) for pelvic lymph node metastasis, ammonia showed increased tracer uptake while ^{18}F-FDG was negative (red arrows); (c) transaxial images of ammonia PET/CT (upper row) and ^{18}F-FDG PET/CT (lower row) for osteogenic metastases, they both showed high uptake.

Fig. 5

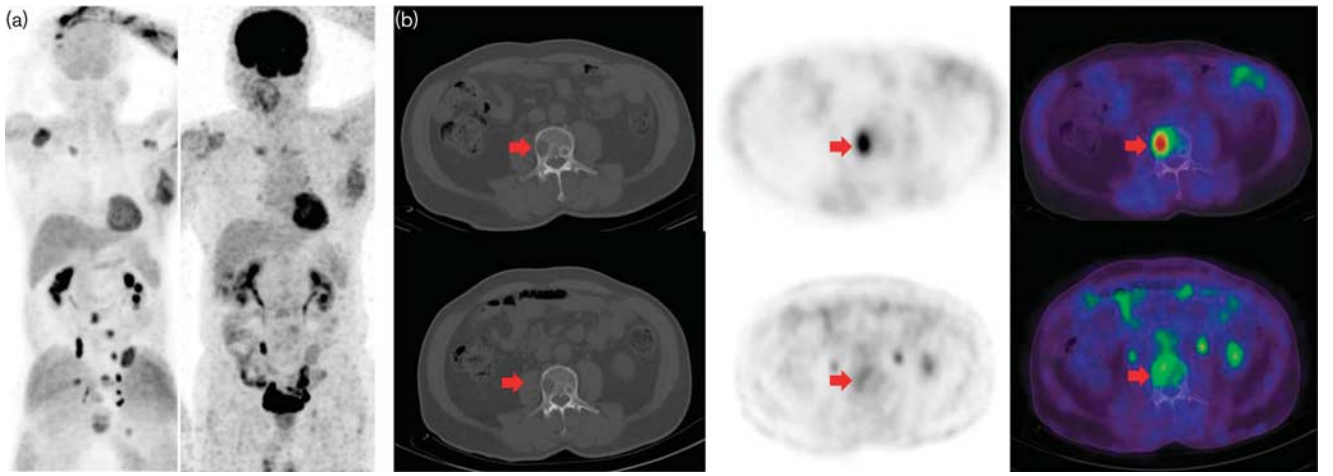

A 60-year-old prostate cancer patient (case 1) with bone metastases: (a) whole-body anterior maximal intensity projection images of ^{13}N-ammonia PET/CT (left column) and ^{18}F-fluorodeoxyglucose (^{18}F-FDG) PET/CT (right column); (b) transaxial images of ammonia PET/CT (upper row) and ^{18}F-FDG PET/CT (lower row) for osteolytic metastasis, although they were both positive (red arrows), ammonia had more accumulation than ^{18}F-FDG.

lower uptake of ^{13}N-ammonia was seen in the setting of inflammation and infection.

In the patient-based analysis, both imaging modalities were able to detect bone metastases. (Figure 5 shows a 60-year-old PC patient with bone metastases.) Meanwhile, the results were similar in the lesion-based analysis. Both for osteogenic and osteolytic lesions, ammonia and ^{18}F-FDG had similar positive rates (97.4 vs. 91.3% for osteogenic lesions; both 100% for osteolytic lesions). Some other PET tracers also suggested for the assessment of PC with bone metastases include ^{18}F-fluoride and ^{18}F-fluorocholine [20, 28], but they were not used to make a distinction between the osteogenic and osteolytic lesions. We found that ^{13}N-ammonia and ^{18}F-FDG are more sensitive in osteolytic lesions than in osteogenic lesions, and ^{13}N-ammonia is more sensitive than ^{18}F-FDG in osteogenic lesions, although there was no significant difference between the two methods. Nevertheless, whether in osteogenic lesions or in osteolytic lesions, the TBR values for ammonia were lower than those for ^{18}F-FDG. This might indicate that the radiation-absorbed doses in tumors for ^{13}N-ammonia are less than those of ^{18}F-FDG. This might be associated with abnormal glutamine metabolism after bone destruction. However, the mechanism about the usefulness of ^{13}N-ammonia in bone metastases is still not yet fully understood and further study needs to be done.

The current results demonstrated close agreement between ^{18}F-FDG and ammonia PET/CT. They showed us that ^{13}N-ammonia and ^{18}F-FDG have similar uptake in PC cells either on glutamine metabolism or on glucose metabolism. It is suggested that ^{13}N-ammonia is a potential PET tracer for detecting distant metastases in PC and is a complement to ^{18}F-FDG for detecting advanced primary PC. However, the diagnosis of primary PC using PET imaging remains a dilemma that warrants further research.

Our study has several limitations. First of all, clinical follow-up instead of histopathology was used in patients as reference for the patient's LN and bone status. In addition, we had collected a small sample of advanced PC cases, and these results need further validation by prospective studies with larger sample size. Further studies are needed to confirm the clinical utility of ^{13}N-ammonia imaging in PC.

Conclusion

The data obtained in this preliminary investigation suggest a clinical impact of ^{13}N-ammonia PET/CT in advanced PC patients as well as of ^{18}F-FDG. ^{13}N-Ammonia is a useful PET tracer for detecting distant metastases in PC, and is a complement to ^{18}F-FDG for detecting advanced primary PC. The combination of these two tracers on the same day can accurately detect advanced PC.

Acknowledgements

The authors thank Professor Ganghua Tang for advice and suggestions on the production of ^{13}N-ammonia. They are also grateful to our staff for their technical assistance and commitment.

This work was supported by National Natural Science Foundation of China (81271599).

Conflicts of interest

There are no conflicts of interest.

References

1 Siegel R, Ma J, Zou Z, Jemal A. Cancer statistics, 2014. *CA Cancer J Clin* 2014; **64**:9–29.

2 Kessler B, Albertsen P. The natural history of prostate cancer. *Urol Clin North Am* 2003; **30**:219–226.

3 Schöder H, Larson SM. Positron emission tomography for prostate, bladder, and renal cancer. *Semin Nucl Med* 2004; **34**:274–292.

4 Thompson IM, Pauler DK, Goodman PJ, Tangen CM, Lucia MS, Parnes HL, *et al*. Prevalence of prostate cancer among men with a prostate-specific antigen level < or =4.0 ng per milliliter. *N Engl J Med* 2004; **350**:2239–2246.

5 Jadvar H. Molecular imaging of prostate cancer: PET radiotracers. *Am J Roentgenol* 2012; **199**:278–291.

6 Avril N, Dambha F, Murray I, Shamash J, Powles T, Sahdev A. The clinical advances of fluorine-2-D-deoxyglucose-positron emission tomography/computed tomography in urological cancers. *Int J Urol* 2010; **17**:501–511.

7 Jadvar H. Molecular imaging of prostate cancer with ^{18}F-fluorodeoxyglucose PET. *Nat Rev Urol* 2009; **6**:317–323.

8 Sung J, Espiritu JI, Segall GM, Terris MK. Fluorodeoxyglucose positron emission tomography studies in the diagnosis and staging of clinically advanced prostate cancer. *BJU Int* 2003; **92**:24–27.

9 Minamimoto R, Uemura H, Sano F, Terao H, Nagashima Y, Yamanaka S, *et al*. The potential of FDG-PET/CT for detecting prostate cancer in patients with an elevated serum PSA level. *Ann Nucl Med* 2011; **25**:21–27.

10 Shiiba M, Ishihara K, Kimura G, Kuwako T, Yoshihara H, Sato H, *et al*. Evaluation of primary prostate cancer using ^{11}C-methionine-PET/CT and ^{18}F-FDG-PET/CT. *Ann Nucl Med* 2012; **26**:138–145.

11 Kitajima K, Murphy RC, Nathan MA, Sugimura K. Update on positron emission tomography for imaging of prostate cancer. *Int J Urol* 2014; **21**:12–23.

12 Clark JC, Aigbirhio FI. Chemistry of nitrogen-13 and oxygen-15. In: Welch MJ, Redvanly CS, editors. *Handbook of radiopharmaceuticals: radiochemistry and applications*. Chichester, West Sussex, UK: John Wiley & Sons Inc.; 2003. pp. 119–140.

13 Cooper AJ. ^{13}N as a tracer for studying glutamate metabolism. *Neurochem Int* 2011; **59**:456–464.

14 Schelstraete K, Simons M, Deman J, Vermeulen FL, Slegers G, Vandecasteele C, *et al*. Uptake of ^{13}N-ammonia by human tumours as studied by positron emission tomography. *Br J Radiol* 1982; **55**:797–804.

15 Xiangsong Z, Weian C, Dianchao Y, Xiaoyan W, Zhifeng C, Xiongchong S. Usefulness of (13)N-NH (3) PET in the evaluation of brain lesions that are hypometabolic on (18)F-FDG PET. *J Neurooncol* 2011; **105**:103–107.

16 Shi X, Zhang X, Yi C, Wang X, Chen Z, Zhang B. The combination of ^{13}N-ammonia and ^{18}F-FDG in predicting primary central nervous system lymphomas in immunocompetent patients. *Clin Nucl Med* 2013; **38**:98–102.

17 Shi X, Zhang X, Yi C, Liu Y, He Q. [^{13}N]Ammonia positron emission tomographic/computed tomographic imaging targeting glutamine synthetase expression in prostate cancer. *Mol Imaging* 2014; **13**:1–10.

18 Buchegger F, Garibotto V, Zilli T, Allainmat L, Jorcano S, Vees H, *et al*. First imaging results of an intraindividual comparison of (11)C-acetate and (18)F-fluorocholine PET/CT in patients with prostate cancer at early biochemical first or second relapse after prostatectomy or radiotherapy. *Eur J Nucl Med Mol Imaging* 2014; **41**:68–78.

19 Heck MM, Souvatzoglou M, Retz M, Nawroth R, Kübler H, Maurer T, *et al*. Prospective comparison of computed tomography, diffusion-weighted magnetic resonance imaging and [^{11}C]choline positron emission tomography/computed tomography for preoperative lymph node staging in prostate cancer patients. *Eur J Nucl Med Mol Imaging* 2014; **41**:694–701.

20 Beheshti M, Vali R, Waldenberger P, Fitz F, Nader M, Loidl W, *et al*. Detection of bone metastases in patients with prostate cancer by ^{18}F fluorocholine and ^{18}F fluoride PET-CT: a comparative study. *Eur J Nucl Med Mol Imaging* 2008; **35**:1766–1774.

21 Mullen AR, Wheaton WW, Jin ES, Chen PH, Sullivan LB, Cheng T, *et al*. Reductive carboxylation supports growth in tumour cells with defective mitochondria. *Nature* 2011; **481**:385–388.

22 Fendt SM, Bell EL, Keibler MA, Davidson SM, Wirth GJ, Fiske B, *et al*. Metformin decreases glucose oxidation and increases the dependency of prostate cancer cells on reductive glutamine metabolism. *Cancer Res* 2013; **73**:4429–4438.

23 Csibi A, Fendt SM, Li C, Poulogiannis G, Choo AY, Chapski DJ, *et al*. The mTORC1 pathway stimulates glutamine metabolism and cell proliferation by repressing SIRT4. *Cell* 2013; **153**:840–854.

24 Gurel B, Iwata T, Koh CM, Jenkins RB, Lan F, Van Dang C, *et al*. Nuclear MYC protein overexpression is an early alteration in human prostate carcinogenesis. *Mod Pathol* 2008; **21**:1156–1167.

25 Pissimissis N, Papageorgiou E, Lembessis P, Armakolas A, Koutsilieris M. The glutamatergic system expression in human PC-3 and LNCaP prostate cancer cells. *Anticancer Res* 2009; **29**:371–377.

26 Lockwood AH. Absorbed doses of radiation after an intravenous injection of N-13 ammonia in man: concise communication. *J Nucl Med* 1980; **21**:276–278.

27 Fucci L, Oliver CN, Coon MJ, Stadtman ER. Inactivation of key metabolic enzymes by mixed-function oxidation reactions: possible implication in protein turnover and ageing. *Proc Natl Acad Sci USA* 1983; **80**:1521–1525.

28 Even-Sapir E, Metser U, Mishani E, Lievshitz G, Lerman H, Leibovitch I. The detection of bone metastases in patients with high-risk prostate cancer: ^{99m}Tc-MDP planar bone scintigraphy, single- and multi-field-of-view SPECT, ^{18}F-fluoride PET, and ^{18}F-fluoride PET/CT. *J Nucl Med* 2006; **47**:287–297.